Acta Crystallographica Section D
Biological Crystallography
ISSN 0907-4449

Physical estimation of triplet phases from two new proteins

F. Mo,[a]* R. H. Mathiesen,[a] P. M. Alzari,[b] J. Lescar[c]† and B. Rasmussen[d]

[a]Institutt for Fysikk, Norges Teknisk-Naturvitenskapelige Universitet, N-7491 Trondheim, Norway, [b]Institut Pasteur, Unité de Biochimie Structurale, 25 Rue du Dr Roux, F-75724 Paris CEDEX 15, France, [c]ESRF, Experiments Division, BP 220, F-38043 Grenoble CEDEX, France, and [d]EMBL Grenoble Outstation, 6 rue Jules Horowitz, BP1 56, F-38042 Grenoble CEDEX, France

† Present address: School of Biological Sciences, Nanyang Technological University, Nanyang Walk, Blk 5, Level 3, Singapore 637616.

Correspondence e-mail: fmo@phys.ntnu.no

Received 11 March 2002
Accepted 9 July 2002

Three-beam interference experiments have been performed with crystals of two glycosidases: guinea-fowl hexagonal lysozyme, MW 14.3 kDa, and *C. thermocellum* endoglucanase CelA, MW 40 kDa. In both cases triplet phases could be estimated. Experimental parameters and details of the procedure are presented along with some examples of the results. The average differences between the estimated phases and those calculated from the crystallographic refinements were 17.9 and 15.9°, respectively. A brief discussion of alternative methods for physical phase acquisition is given, including possible strategies for the measurement and application of experimental phases in macromolecular crystallography.

1. Introduction

Diffraction in a crystal at or very close to a multiple-beam situation can provide information on sums of structure-factor phases. This direct physical extraction of phase information has been demonstrated with crystals over a wide range of molecular complexity, including proteins.

Physical phase estimation by three-beam interference in a protein crystal was first reported for myoglobin (Hümmer *et al.*, 1991). At about the same time, phase effects were also observed with crystals of oxyhaemoglobin (Chang *et al.*, 1991). In the following years, evidence for multi-beam interference or actual phase estimation has been demonstrated for a few other proteins: catalase oxidoreductase (Weckert *et al.*, 1993), tetragonal lysozyme (Weckert *et al.*, 1993, 1999; Chang *et al.*, 1999; Shen, 1998; Shen *et al.*, 2000), triclinic lysozyme (Weckert & Hümmer, 1997; Weckert *et al.*, 1999), proteinase K (Weckert *et al.*, 1999) and T2A–Im7, a protein complex (Chang *et al.*, 1999). In addition, some other proteins have yielded triplet phases in exploratory three-beam diffraction experiments: nettle lectin, a Fab-fragment, trypsin and hisf1 (Weckert, 2000). The unit-cell volumes of these proteins range from about 66 800 Å^3 (myoglobin) to 1.2 × 10^6 Å^3 (catalase).

The first experiments were primarily feasibility studies: can phase information be obtained from three-beam diffraction experiments in protein crystals? With this question affirmed, one natural next question relates to the applicability of such phases. Clearly, the potential for physically estimated triplet phases (PETPs) in macromolecular crystallography depends critically on their general availability. In addition to crystal mosaicity, which is a major impediment to physical phase estimation in non-perfect crystals, there are several limiting factors. There is the general weak scattering power, a densely populated reciprocal lattice creating multiple excitations

overlapping with the three-beam case under study and the limited lifetime of a crystal in an X-ray beam. At present about ten proteins have yielded triplet phases or have at least shown significant phase effects under three-beam diffraction conditions. We report here physical phase estimation (PPE) with crystals of two glycosidase proteins, guinea-fowl hexagonal lysozyme (MW 14.3 kDa) and *C. thermocellum* endoglucanase CelA (MW 40 kDa). Reports on this work have been presented (Mo *et al.*, 1997, 1998).

2. Physical phase estimation

2.1. General considerations

With a six-circle Eulerian diffractometer, a primary reflection H can be carried into the horizontal plane and a scan is then made about the primary scattering vector $\mathbf{H}$ (Ψ-scan). The profile of the primary diffracted intensity $I_{\mathbf{H}}$ is recorded as a second reciprocal-lattice node L is rotated through the Ewald sphere. Interference between the incident beam and the two excited beams takes place through a multiple scattering process and gives rise to a perturbation of $I_{\mathbf{H}}$, from which information on the associated triplet phase $\Phi_3 = \varphi_{-\mathbf{H}} + \varphi_{\mathbf{L}} + \varphi_{\mathbf{H}-\mathbf{L}}$ can be obtained. A triplet phase is a structure invariant independent of the choice of origin. The phase information is projected out in the profile as characteristic antisymmetric $(\cos\Phi_3)/\alpha_{\mathbf{L}}$ and symmetric $(\sin\Phi_3)/\alpha_{\mathbf{L}}^2$ features about the exact three-beam point, where *the excitation error* $\alpha_{\mathbf{L}} = 0$, allowing phases to be estimated with a mean error about 20° or less. The experiment involves measurement of pairs of triplets $-H/L/H-L$ with phase Φ_3 and $H/-L/-H+L$ with phase $-\Phi_3$. Assuming a simple reversal of beam paths through the crystal in the two cases, the phase-independent contributions (*Umweganregung*/*Aufhellung*) are identical, yielding the phase information from a comparison of the two interference profiles.

Prerequisites for the present work are a high-flux unfocused synchrotron beam with small beam divergency, also tunable in energy, and a high-precision six-circle diffractometer with very high angular resolution allowing a pure rotation about the primary diffraction vector, the Ψ-scan.

2.2. Interpretation of phase

The three-beam perturbation of the two-beam kinematical intensity $I_{\mathbf{H}}$ has been derived in analytical form for a perfect crystal of finite size and for certain scattering geometries (Thorkildsen, 1987; Thorkildsen & Larsen, 1998) from a solution of the Takagi–Taupin equations (Takagi, 1962, 1969; Taupin, 1964). The three-beam intensity $I_{3,\mathbf{H}}$ can be rewritten in a simplified form which brings out the terms that are most important for the phase estimation (Mathiesen *et al.*, 1998),

$$I_{3,\mathbf{H}}/I_{\mathbf{H}} \propto 1 - 2(CR_F)[(\cos\Phi_3)f_2(u) + (\sin\Phi_3)f_1(u)] + (CR_F)^2[2f_3(u) - (|F_{\mathbf{L}}|^{-2} + |F_{\mathbf{H}-\mathbf{L}}|^{-2})|F_{\mathbf{H}}|^2 f_1(u)]. \quad (1)$$

C is a dimensionless constant, R_F is a ratio of structure-factor amplitudes,

$$R_F = |F_{\mathbf{L}}||F_{\mathbf{H}-\mathbf{L}}|/|F_{\mathbf{H}}|, \quad (2)$$

$f_1(u) = (1/u^2)(1 - \cos u)$, $f_2(u) = (1/u)[1 - (\sin u)/u]$ and $f_3(u) = (1/u)f_2(u)$ are functions of a dimensionless excitation error, $u = 2\pi l\alpha_{\mathbf{L}}$, where l is a typical perfect crystal domain dimension and $\alpha_{\mathbf{L}} = k_{\mathbf{L}} - K$; $k_{\mathbf{L}}$ and K are the wavevector magnitudes of the secondary beam and the incident beam, respectively, inside the crystal. Thus, α_{L} and therefore also u are negative when L is inside the Ewald sphere and positive when it is outside; $f_1(u)$ and $f_3(u)$ are non-negative and symmetrical about $u = 0$, where they have global maxima, $f_2(u)$ is antisymmetrical about $u = 0$, with $f_2(0) = 0$ and with sign as u itself. The phase information lies in the second term of (1). If $\Phi_3 \simeq 0/\pi$, $f_2(u)$ will project out the phase-dependent perturbation as an asymmetry in the intensity profile near the exact three-beam point. This is the only asymmetric term in (1); therefore, asymmetry features in the intensity profile must be related to Φ_3. If $\Phi_3 \simeq \pm\pi/2$ the perturbation will be symmetric with an extremum at $u = 0$; the antisymmetry of the sine itself gives a maximum for $\Phi_3 = -\pi/2$ and a minimum for $\Phi_3 = \pi/2$. The profile for a general Φ_3 will be a characteristic composition of these extreme features (see, for example Weckert *et al.*, 1993). The last term of (1) contains the phase-independent contributions which include both *Umweganregung* and *Aufhellung* effects. For a more detailed discussion of (1) and the nature of the approximations involved, we refer to Mathiesen *et al.* (1998).

There exist alternate theoretical descriptions of three-beam perturbation of a two-beam intensity. They are based on the so-called fundamental equations of wavefields in dynamical X-ray diffraction, either accessed *via* a second-order Born approximation (Chang & Tang, 1988; Chang *et al.*, 1989; Shen, 1986, 1999; Stetsko *et al.*, 2000) or through numerical solution of the fundamental equation eigenvalues (Colella, 1974; Chang, 1984; Weckert & Hümmer, 1990, 1997). For an overview of the various theoretical lines of approach, see Thorkildsen *et al.* (2001). In all theories based on the fundamental equations the scattering medium is treated as a semi-infinite plane-parallel perfect crystal; thus, the influence of crystal shape and beam-path lengths within the crystal on the multiple diffraction intensity cannot be properly assessed. This is also the case for relation (1). The complementarity and ranges of validity of various theoretical descriptions of three-beam diffraction have been examined in recent studies (Thorkildsen *et al.*, 2001; Thorkildsen & Larsen, 2002).

3. The proteins

Triplet phases were estimated for two glycosidases, guinea-fowl hexagonal lysozyme (GFHL) and *C. thermocellum* cellulase (CelA).

3.1. Guinea-fowl hexagonal lysozyme (GFHL)

The structure of this protein, which is closely related to hen lysozyme, has been determined at 1.9 Å resolution (Lescar *et al.*, 1994). It crystallizes in space group $P6_122$, with unit-cell parameters redetermined as $a = b = 89.02$, $c = 61.80$ Å and

unit-cell volume $V \simeq 424\,100$ Å^3. The crystals generally had low mosaicity, but all specimens that were examined consisted of more than one crystal block. The crystal used for the phase measurements was a twin; the full-width at half-maximum (FWHM) values for the larger individual from ω rocking curves were in the range 0.004–0.010°. Two intensity profiles showing splitting of different magnitude are reproduced in Fig. 1. Three-beam interference profiles were collected by repeated Ψ-scans for 28 pairs of triplets $-H/L/H-L$ and $H/-L/-H+L$. From these profiles, 20 triplet phases could be estimated. We ascribe the reduction in number primarily to twinning causing multiple overlap of interference maxima, thus obscuring the phase information in the profile. Three examples of experimental profile pairs are shown in Fig. 2.

3.2. *C. thermocellum* cellulase (CelA)

Endoglucanase CelA (40 kDa) is an extracellular glycosidase which is part of the cellulosome, a multi-enzymatic complex which is very active in degrading natural cellulose. CelA crystallizes in the orthorhombic space group $P2_12_12_1$, with unit-cell parameters $a = 50.05$, $b = 63.50$, $c = 104.75$ Å, $V \simeq 333\,000$ Å^3. Its crystal structure has been determined by the MIR technique and refined with data at 1.65 Å resolution (Alzari *et al.*, 1996). The structure of CelA in complex with a substrate has been refined to atomic resolution (0.94 Å) and a report on this work has recently been published (Guerin *et al.*, 2002).

Two prismatic crystals with well developed faces and physical dimensions 1.2 × 0.24 × 0.21 mm and 1.1 × 0.22 × 0.14 mm were used for the triplet-phase measurements. Both crystals had small mosaicity; FWHM values from ω rocking curves were in the range 0.006–0.015°. Three-beam interference profiles were collected by repeated Ψ-scans for 49 pairs of triplets. Four pairs of these intensity profiles could not be interpreted owing to an insufficient intensity perturbation. Of the remaining 45 profiles, five were estimated twice, thus rendering 40 unique triplet-phase values. Three experimental profile pairs are shown in Fig. 3.

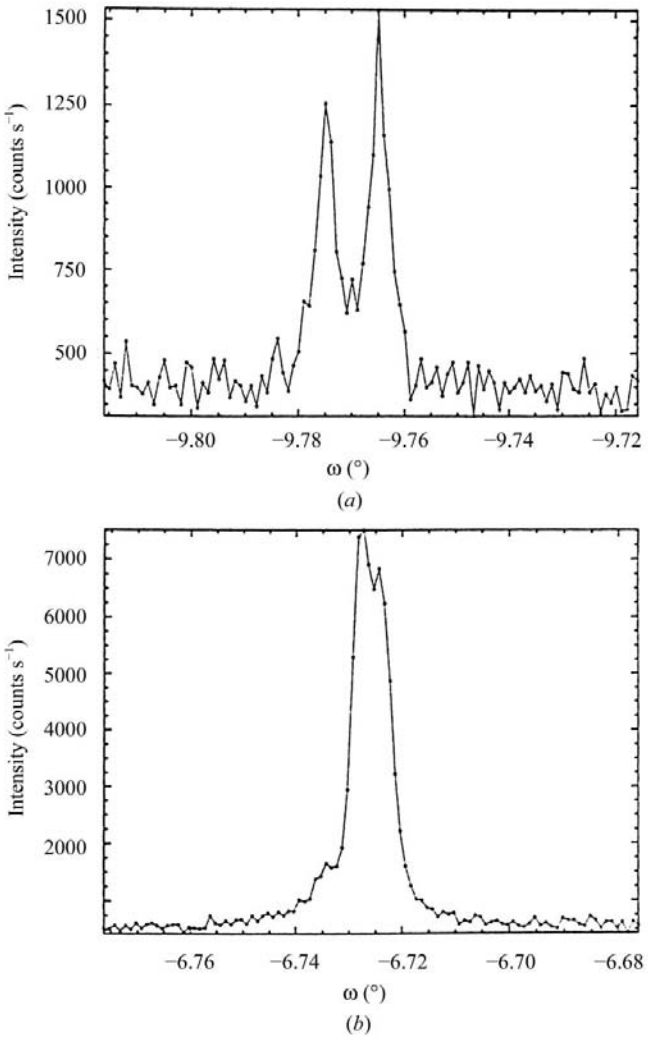

Figure 1
GFHL. Intensity profiles from ω scans of the reflections (*a*) 2 −27 0 and (*b*) 17 −10 −8.

4. Experimental

The three-beam diffraction experiments were carried out on a six-circle Huber diffractometer (Hümmer *et al.*, 1987, 1989) at the time located on the Swiss–Norwegian Beamlines (SNBL), station A at ESRF. An unfocused beam, slitted down to about 0.7 × 0.7 mm was used on the sample, which was located 16.7 m from a double-crystal Si(111) monochromator and 47.5 m from the bending-magnet source. The beam divergencies at the sample position, including the angular acceptance of the monochromator, are about 25 µrad horizontally and vertically at $\lambda = 1.0$ Å. The energy resolution of the monochromatic beam is $\Delta\lambda/\lambda \simeq 1.3 \times 10^{-4}$. The resolution in the diffractometer axes was 5×10^{-5}° in ω, 1×10^{-4}° in Ψ and 2×10^{-4}° in φ and χ. In the first work with hexagonal lysozyme, a constant wavelength of $\lambda = 1.200$ Å was used for all measurements. This was because of a temporary inability to calculate optimized wavelengths for the purpose of minimizing or avoiding measurable interferences from other strong secondary reflections closely adjacent to the Ewald sphere. The results from these measurements suggested that this procedure was not limiting the phase acquisition and therefore in the study of CelA we continued to use a constant $\lambda = 1.200$ Å in all the Ψ-scans. The profiles were scanned 5–100 times, depending on the scattering power of the primary reflection H and the magnitude of the perturbations from the interference terms. The Ψ-scan width was varied from ±0.035 to ±0.04° from the three-beam point with step size in the range 0.0003 to 0.0005°; these parameters were adjusted according to the width and strength of the interference profile.

5. Results

Phases were estimated independently by two researchers and averaged. The general accuracy attempted was 22.5°, except near ±90° where a more accurate estimate is feasible as the asymmetry of the intensity profile is reversed crossing over these points. As an example of the agreement in the phase

assignments, we note that in the work with CelA there were 45 interpreted intensity profiles; of these, 32 were ascribed identical phase, four differed by about 10° and nine by 22.5°.

We now describe in some detail the interpretation of features in the interference profiles leading to an assignment of phase. In Fig. 2 (GFHL) and Fig. 3 (CelA) both members of some Friedel-related pairs are shown; the profile to the left in each pair corresponds to the triplet $-H/L/H - L$, with the estimated triplet-phase value $\Phi_3^{\rm est}$ given in this figure. In the legend of these figures the indices $-H/L/H - L$ of the three

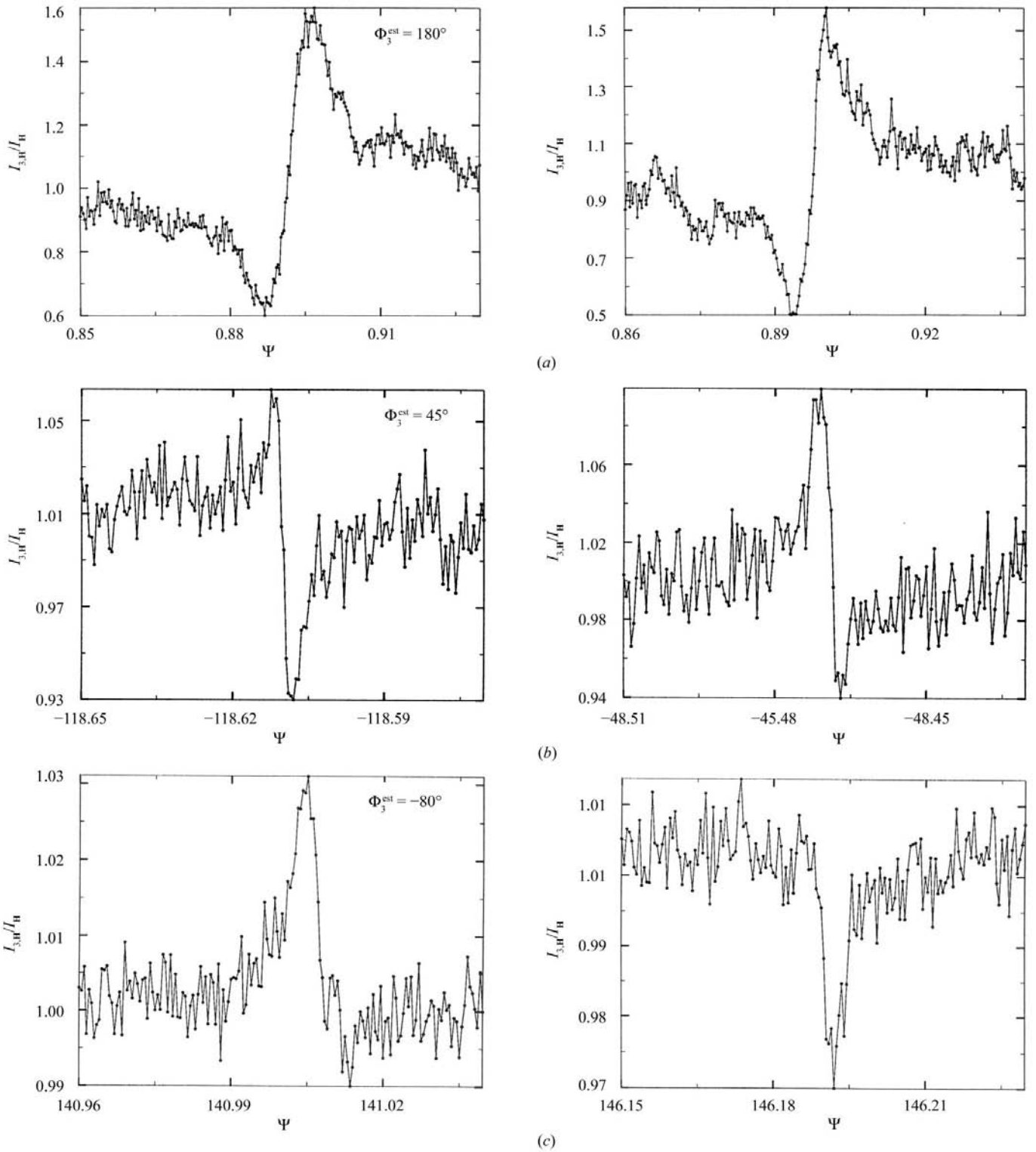

Figure 2
GFHL. Ψ-scans of three pairs of interference profiles: the estimated triplet phase $\Phi_3^{\rm est}$ is given in the left profile of each pair. (*a*) Triplet 2 2 1/−1 −1 0/ −1 −1 −1, $\Phi_3^{\rm calc} = 180°$. (*b*) Triplet 14 3 8/−2 1 0/ −12 −4 −8, $\Phi_3^{\rm calc} = 48°$. (*c*) Triplet 21 2 8/−1 −1 0/20 1 8, $\Phi_3^{\rm calc} = -56°$.

structure factors involved in the triplet are given along with the triplet phase calculated from the single phases obtained in the crystallographic refinement of the structure, Φ_3^{calc}.

Fig. 2(*a*) shows that both profiles have a strong depression for $\Delta\Psi < 0$ ($\alpha_{\mathbf{L}} < 0$) near the three-beam point $\Delta\Psi = 0$, characteristic for a π-type Φ_3. The magnitudes of the extrema

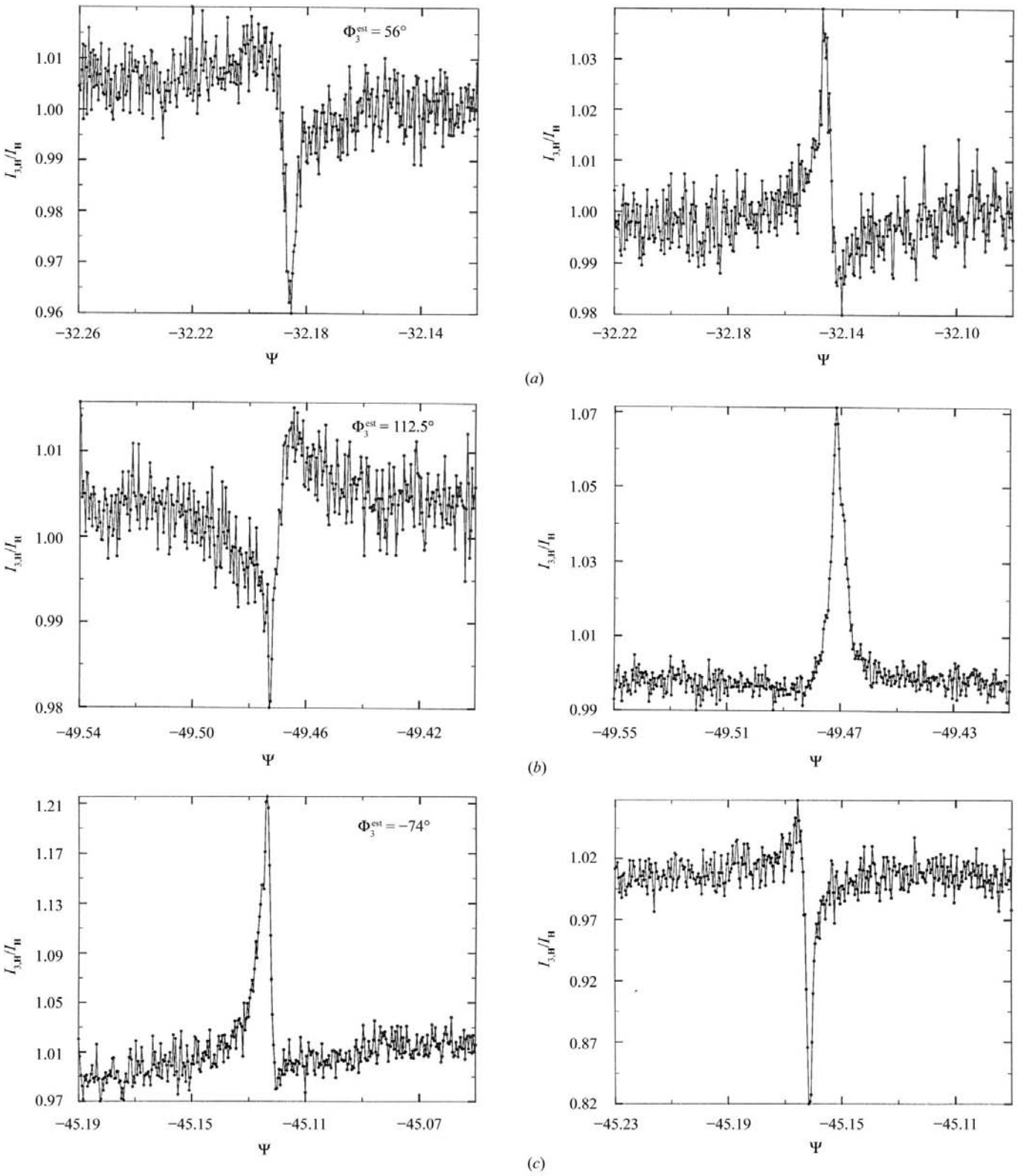

Figure 3
CelA. Ψ-scans of three pairs of interference profiles: the estimated triplet phase Φ_3^{est} is given in the left profile of each pair. (*a*) Triplet 8 9 26/−7 −5 −20/−1 −4 −6, $\Phi_3^{calc} = 43°$. (*b*) Triplet 14 1 8/−14 0 −10/0 −1 2, $\Phi_3^{calc} = 117°$. (*c*) Triplet 7 5 16/−7 −5 −20/0 0 4, $\Phi_3^{calc} = -64°$.

relative to the two-beam level are very similar, leading to a phase assignment of 180°. In the backgrounds on either side of the main features there are signs of interference with other adjacent secondary reflections L and probably also contributions from the minor twin, but they do not compromise the phase estimate. Another example is shown in Fig. 2(*c*). The left profile shows a peak and the one to the right has a trough of the same magnitude, which indicates a triplet of the $\pm\pi/2$ type, the left one being associated with the negative sign. However, in both profiles there is a slight depression in the background for $\Delta\Psi > 0$ ($\alpha_{\mathbf{L}} > 0$), which is the signature of a small amount of zero character. This places the triplet phases in quadrants 4 and 1, respectively; the averaged estimated phase was -80°. As one example from the measurements on crystals of CelA, we take the profile pair in Fig. 3(*a*). Both profiles have a clear zero-type depression for $\Delta\Psi > 0$; the smaller magnitude of the constructive interference in the left profile shows that it belongs to phase quadrant 1 and that the Friedel partner to the right is in quadrant 4. A closer examination of the magnitudes of the extreme departures from the two-beam level led to the averaged phase estimate of 56°.

The average difference, $\langle\Delta\Phi_3\rangle$, between the N estimated unique triplet phases and those calculated from the crystallographic refinements was 17.9° for GFHL ($N = 20$) and 15.9° for CelA ($N = 40$). The differences are in the expected range for PPE based on sequential measurements of three-beam interference profiles.

We note that both proteins are remarkably resistant to X-rays; there were only slight changes in the intensity profiles of some of the test reflections even after about 20 h of exposure. Both in terms of lifetime in the beam and crystal mosaicity they would be excellent candidates for structure determination based on PPE.

6. Discussion

The experimental limitations and the actual procedure for PPE by sequential acquisition of triplet phases using a six-circle diffractometer and a point detector are now quite well established. With respect to the application of experimental phases for solving macromolecular structure, some important questions need further study. The first relates to the execution of such measurements. Alternative and interrelated experimental techniques have been proposed and demonstrated: the reference-beam method (Shen, 1998; Shen *et al.*, 2000) and the stereoscopic multibeam imaging method (Chang *et al.*, 1999). Both methods employ an oscillating-crystal technique: oscillatory Ψ-scans are performed about the diffraction vector $\mathbf{L}$ for a common secondary reflection L, allowing a multitude of primary reflections H_i to interfere with L. The resulting intensity profiles $I_{\mathbf{H}i}$ are recorded *versus* $\Delta\theta_{\mathbf{L}}$ with an area detector, $\Delta\theta_{\mathbf{L}}$ being the tilt angle from the exact Bragg position for the L reflection. The primary advantage of these methods is that a large number of intensity profiles can be collected in a short time; the disadvantage at present is the lower accuracy of the phase assignment compared with the point-detector method. Of some 500 three-beam interference profiles collected with the reference-beam method for a crystal of tetragonal lysozyme, about 1/3 of the triplet phases obtained from an automatic phase assignment procedure had errors exceeding 90° (Shen *et al.*, 2000). Chao *et al.* (2002) have reported an average difference of $\leq 30^{\circ}$ between estimated and calculated triplet-phase values for a large number of measured profiles also from tetragonal lysozyme. With improved angular resolution and more refined discriminatory criteria for the acceptance of phases, these methods appear to have potential in work with macromolecular structures (Weeks *et al.*, 2000).

Another important question pertains to the strategy for measurement and application of phases: *which* triplets to estimate and *how* to obtain a structure solution most efficiently from a minimal number of estimated phases. With a protein, triplets can be chosen so as to contain a small number of frequently recurring strong reflections at very low resolution. Thus, 30 of the 40 unique triplets studied for CelA include one of the reflections 110, 111, 012, 200 and 004, corresponding to the resolution range 25–40 Å. Reflections at such low resolution are not commonly measured in crystallographic work, although they contain information on the coarse structure, including the solvent. This information may be important and can be retained in the data for the identification of the molecular envelope. Moreover, they participate in many physically accessible three-phase structure invariants and are therefore very useful in PPE at low resolution. One strategy for the interference measurements involves work with linked sequences of triplets, designed to render single phases in succession once a small starting set including reflections for fixing the origin and enantiomorph has been selected (Mathiesen & Mo, 1997*a*,*b*). Computational extension of this enlarged starting set can be effected, for example, by maximum entropy (Bricogne, 1984, 1988; Bricogne & Gilmore, 1990; Prince *et al.*, 1988; Doublié *et al.*, 1994; Gilmore, 1996) or maximum-likelihood methods (Stuart & Ord, 1991; Pannu & Read, 1996; Murshudov *et al.*, 1997; Lunin *et al.*, 1998; Pannu *et al.*, 1998; Petrova *et al.*, 2000). Methods based on wavelet analysis (Combes *et al.*, 1989; Main & Wilson, 2000, Lunin, 2000) or discrete Hilbert transforms (Zanotti *et al.*, 1996) are perhaps better suited to explore the archipelagic structure of the accumulated phase information in reciprocal space. Once a molecular envelope has been identified and improved from an extended set of phases, several techniques exist for further phase extension and refinement, by modification (filtering) in real space or in reciprocal space or in both spaces combined.

The authors thank Professor Edgar Weckert, HASYLAB and Professor Kurt Hümmer of the University of Karlsruhe for the use of their six-circle Huber diffractometer. We are indebted to ESRF for allocation of beamtime (Experiments MI-166 and MI-209) as well as to the Swiss–Norwegian Beamlines (SNBL) at ESRF (Experiment 1–02-65) and the beamline staff for unfailing support. Financial support from

Norges Forskningsråd (NFR) under Grant 101166/431 is gratefully acknowledged.

References

Alzari, P. M., Souchon, H. & Dominguez, R. (1996). *Structure*, **4**, 265–275.

Bricogne, G. (1984). *Acta Cryst.* A**40**, 410–445.

Bricogne, G. (1988). *Acta Cryst.* A**44**, 517–545.

Bricogne, G. & Gilmore, C. J. (1990). *Acta Cryst.* A**46**, 284–297.

Chang, S.-L. (1984). *Multiple Diffraction of X-rays in Crystals.* Berlin: Springer–Verlag.

Chang, S.-L., Chao, C.-H., Huang, Y.-S., Jean, Y.-C., Sheu, H.-S., Liang, F.-J., Chien, H.-C., Chen, C.-K. & Yuan, H. S. (1999). *Acta Cryst.* A**55**, 933–938.

Chang, S.-L., Huang, M.-T., Tang, M.-T. & Lee, C.-H. (1989). *Acta Cryst.* A**45**, 870–878.

Chang, S.-L., King, H. E., Huang, M.-T. & Gao, Y. (1991). *Phys. Rev. Lett.* **67**, 3113–3116.

Chang, S.-L. & Tang, M.-T. (1988). *Acta Cryst.* A**44**, 1065–1072.

Chao, C.-H., Hung, C.-Y., Huang, Y.-S., Ching, C.-H., Lee, Y.-R., Jean, Y.-C., Lai, S.-C., Stetsko, Y. P., Yuan, H. & Chang, S.-L. (2002). *Acta Cryst.* A**58**, 33–41.

Colella, R. (1974). *Acta Cryst.* A**30**, 413–423.

Combes, J. M., Grossmann, A. & Tchamitchian, P. (1989). Editors. *Wavelets.* Berlin: Springer–Verlag.

Doublié, S., Xiang, S., Gilmore, C. J., Bricogne, G. & Carter, C. W. Jr (1994). *Acta Cryst.* A**50**, 164–182.

Gilmore, C. J. (1996). *Acta Cryst.* A**52**, 561–589.

Guérin, D. M. A., Lascombe, M. B., Costabel, M., Souchon, H., Lamzin, V., Béguin, P. & Alzari, P. M. (2002). *J. Mol. Biol.* **316**, 1061–1069.

Hümmer, K., Bondza, H. & Weckert, E. (1987). *Acta Cryst.* A**43**, Suppl. C-222.

Hümmer, K., Schwegle, W. & Weckert, E. (1991). *Acta Cryst.* A**47**, 60–62.

Hümmer, K., Weckert, E. & Bondza, H. (1989). *Acta Cryst.* A**45**, 182–187.

Lescar, L., Souchon, H. & Alzari, P. M. (1994). *Protein Sci.* **3**, 788–798.

Lunin, V. Y. (2000). *Acta Cryst.* A**56**, 73–84.

Lunin, V. Y., Lunina, N. L., Petrova, T. E., Urzhumtsev, A. G. & Podjarny, A. D. (1998). *Acta Cryst.* D**54**, 726–734.

Main, P. & Wilson, J. (2000). *Acta Cryst.* D**56**, 1324–1331.

Mathiesen, R. H. & Mo, F. (1997*a*). *Acta Cryst.* D**53**, 262–268.

Mathiesen, R. H. & Mo, F. (1997*b*). *Acta Cryst.* D**53**, 626.

Mathiesen, R. H., Mo, F., Eikenes, A., Nyborg, T. & Larsen, H. B. (1998). *Acta Cryst.* A**54**, 338–347.

Mo, F., Mathiesen, R. H., Alzari, P. M., Lescar, J. & Rasmussen, B. (1997). *Highlights in X-ray Synchrotron Radiation Research, Grenoble, 17–20 November 1997*. Abstracts, p. 107.

Mo, F., Mathiesen, R. H., Alzari, P. M., Lescar, J. & Rasmussen, B. (1998). *18th European Crystallography Meeting (ECM-18), Praha, 15–20 August 1998.* Abstracts, p. 484.

Murshudov, G. N., Vagin, A. A. & Dodson, E. J. (1997). *Acta Cryst.* D**53**, 240–255.

Pannu, N. S., Murshudov, G. N., Dodson, E. J. & Read, R. J. (1998). *Acta Cryst.* D**54**, 1285–1294.

Pannu, N. S. & Read, R. J. (1996). *Acta Cryst.* A**52**, 659–668.

Petrova, T. E., Lunin, V. Y. & Podjarny, A. D. (2000). *Acta Cryst.* D**56**, 1245–1252.

Prince, E., Sjölin, L. & Alenljung, R. (1988). *Acta Cryst.* A**44**, 216–222.

Shen, Q. (1986). *Acta Cryst.* A**42**, 525–533.

Shen, Q. (1998). *Phys. Rev. Lett.* **80**, 3268–3271.

Shen, Q. (1999). *Phys. Rev. Lett.* **83**, 4784–4787.

Shen, Q., Kycia, S. & Dobrianov, I. (2000). *Acta Cryst.* A**56**, 268–279.

Stetsko, Y. P., Juretschke, H. J., Huang, Y.-S., Chao, C.-H., Chen, C.-K. & Chang, S.-L. (2000). *Acta Cryst.* A**56**, 394–400.

Stuart, A. & Ord, K. J. (1991). *Kendall's Advanced Theory of Statistics*, 5th ed., Vol. 2. London/Melbourne/Auckland: Edward Arnold.

Takagi, S. (1962). *Acta Cryst.* **15**, 1311–1312.

Takagi, S. (1969). *J. Phys. Soc. Jpn*, **26**, 1239–1253.

Taupin, D. (1964). *Bull. Soc. Fr. Minéral. Cristallogr.* **87**, 469–511.

Thorkildsen, G. (1987). *Acta Cryst.* A**43**, 361–369.

Thorkildsen, G. & Larsen, H. B. (1998). *Acta Cryst.* A**54**, 120–128.

Thorkildsen, G. & Larsen, H. B. (2002). *Acta Cryst.* A**58**, 252–258.

Thorkildsen, G., Larsen, H. B. & Weckert, E. (2001). *Acta Cryst.* A**57**, 389–394.

Weckert, E. (2000). Personal communication.

Weckert, E., Hölzer, K., Schroer, K., Zellner, J. & Hümmer, K. (1999). *Acta Cryst.* D**55**, 1320–1328.

Weckert, E. & Hümmer, K. (1990). *Acta Cryst.* A**46**, 387–393.

Weckert, E. & Hümmer, K. (1997). *Acta Cryst.* A**53**, 108–143.

Weckert, E., Schwegle, W. & Hümmer, K. (1993). *Proc. R. Soc. London Ser. A*, **442**, 33–46.

Weeks, C. M., Xu, H., Hauptman, H. A. & Shen, Q. (2000). *Acta Cryst.* A**56**, 280–283.

Zanotti, G., Fogale, F. & Capitani, G. (1996). *Acta Cryst.* A**52**, 757–765.